APL Materials

RESEARCH ARTICLE | MARCH 25 2026

Large sub-Kelvin magnetocaloric effect and phase behavior of gadolinium nitrate hexahydrate

David Gracia ; Marc Ubach I Cervera ; Emmanouil K. Charkiolakis ; Inés García-Rubio ; Constantinos J. Milios ; Marco Evangelisti

Check for updates

APL Mater. 14, 031119 (2026)
https://doi.org/10.1063/5.0316768

View Online
Export Citation

Articles You May Be Interested In

Vibrational studies and phase transition in mercury(II) perchlorate hexahydrate

J. Chem. Phys. (November 1983)

Systematics of EPR spectra of Gd^{3+} in rare-earth trinitrate hexahydrate hosts

J. Chem. Phys. (October 1978)

Electron paramagnetic resonance of Fe^{3+} in guanidinium aluminum sulfate hexahydrate

J. Chem. Phys. (November 1976)

10 April 2026 11:20:15

AIP Advances
Why Publish With Us?
21DAYS average time to 1st decision
OVER 4 MILLION views in the last year
INCLUSIVE scope
Learn More
AIP Publishing

AIP Publishing

APL Materials ARTICLE pubs.aip.org/aip/apm

Large sub-Kelvin magnetocaloric effect and phase behavior of gadolinium nitrate hexahydrate

Cite as: APL Mater. 14, 031119 (2026); doi: 10.1063/5.0316768
Submitted: 15 December 2025 • Accepted: 10 March 2026 •
Published Online: 25 March 2026

View Online Export Citation CrossMark

David Gracia,[1] Marc Ubach I Cervera,[1] Emmanouil K. Charkiolakis,[1] Inés García-Rubio,[1] Constantinos J. Milios,[2] and Marco Evangelisti[1,a)]

AFFILIATIONS

[1] Instituto de Nanociencia y Materiales de Aragón (INMA), CSIC—Universidad de Zaragoza, 50009 Zaragoza, Spain
[2] Department of Chemistry, The University of Crete, Voutes, 71003 Herakleion, Greece

[a)] **Author to whom correspondence should be addressed:** evange@unizar.es

ABSTRACT

We report a comprehensive magnetothermal study of the classical gadolinium salt $[Gd(NO_3)_3]\cdot 6H_2O$ at temperatures approaching absolute zero. Despite its long-standing availability as a commercial compound, its magnetocaloric properties have remained unexplored. Using electron paramagnetic resonance, magnetic susceptibility, heat capacity, and direct measurements of the magnetocaloric effect, we reveal that weak dipolar interactions combined with axial crystal-field anisotropy drive antiferromagnetic ordering at $T_N = 0.21$ K. Remarkably, $[Gd(NO_3)_3]\cdot 6H_2O$ exhibits an isothermal magnetic entropy change of $-\Delta S_m = 26.1$ J K^{-1} kg^{-1} at $T = 0.6$ K for a modest field variation of $\Delta B = 1$ T and an adiabatic temperature change of $\Delta T_{ad} = 5.0$ K at $T = 1.6$ K for the same ΔB, placing its performance among the strongest reported for Gd-based refrigerants under comparable low-field and sub-Kelvin conditions. These results provide a reference for understanding magnetocaloric behavior in hydrated salts and highlight the interplay between dipolar coupling and crystal-field anisotropy.

© 2026 Author(s). All article content, except where otherwise noted, is licensed under a Creative Commons Attribution (CC BY) license (https://creativecommons.org/licenses/by/4.0/). https://doi.org/10.1063/5.0316768

10 April 2026 11:20:15

I. INTRODUCTION

The adiabatic demagnetization refrigerator (ADR) operates based on the magnetocaloric effect (MCE), which describes the reversible changes in isothermal magnetic entropy, ΔS_m, and adiabatic temperature, ΔT_{ad}, which occur in magnetocaloric materials under variations of the applied magnetic field, ΔB.[1,2] The ADR was the first technology developed to achieve temperatures approaching absolute zero, nearly a century ago.[3] Since then, it has been widely employed, particularly in situations where the use of cryogenic fluids is impractical.[4,5] For example, ADRs are frequently used in zero-gravity environments to cool down x-ray detectors or sensors onboard space observatories and telescopes. Moreover, recent advances in multi-stage ADR systems, together with the increasing scarcity and high cost of the rare ^{3}He isotope,[6,7] have further increased interest in ADR technology. As a result, modern applications that require sub-Kelvin temperatures, such as quantum devices, are increasingly adopting ADRs to achieve these extreme conditions.[8]

Over the past century, numerous magnetocaloric materials have been investigated for integration into ADR systems operating at the lowest temperatures. The design of efficient refrigerants requires materials that simultaneously exhibit (i) high magnetic density, (ii) low crystal-field anisotropy, and (iii) the absence of magnetic phase transitions at least down to the operational temperature.[9] In this context, the rare-earth ion Gd^{3+} is often favored for cryogenic magnetocaloric applications due to its isotropic $^8S_{7/2}$ electronic ground state, which enables a large MCE that remains significant at very low temperatures. For that reason, a wide range of Gd^{3+}-based compounds have been explored, including $Gd_3Ga_5O_{12}$ (GGG),[10] $GdLiF_4$,[11] $Gd(HCOO)_3$,[12] $GdPO_4$,[13] GdF_3,[14] $GdVO_4$,[15] $Gd(OH)F_2$,[16] $[GdCl_3]\cdot 6H_2O$ and $[Gd_2(SO_4)_3]\cdot 8H_2O$,[17] $\{Gd_2\}$,[18] $\{GdW_{10}\}$ and $\{GdW_{30}\}$,[19] $\{GdZn\}$,[20] $\{Gd_7\}$,[21] Ba_2GdSbO_6 and Sr_2GdSbO_6,[22] $KBaGd(BO_3)_2$,[23] $\{Gd_{12}Na_6\}$,[24] or $Gd_{9.33}[SiO_4]_6O_2$.[25] However, despite the historical relevance of Gd^{3+}-based materials, the magnetothermal and magnetocaloric properties of the classical gadolinium salt $[Gd(NO_3)_3]\cdot 6H_2O$, originally proposed as a refrigerant decades ago[26] and later employed as a precursor for

© Author(s) 2026

synthesizing more complex refrigerants,[27–33] remain largely unexplored. To the best of our knowledge, only a few studies have addressed its magnetic susceptibility (limited to temperatures down to 2 K)[34,35] and its spectroscopic properties.[36]

Herein, we present, for the first time, a comprehensive investigation of the magnetic and magnetocaloric properties of $[Gd(NO_3)_3]\cdot 6H_2O$ at temperatures approaching absolute zero. To complete its physical characterization, we performed measurements on 1% diluted samples of $[R_{0.99}Gd_{0.01}(NO_3)_3]\cdot 6H_2O$ (hereafter denoted as $[Gd@R(NO_3)_3]\cdot 6H_2O$), where R represents various trivalent host ions. Our results reveal that $[Gd(NO_3)_3]\cdot 6H_2O$ undergoes antiferromagnetic ordering at the Néel temperature $T_N = 0.21$ K, driven by dipolar interactions combined with crystal-field anisotropy. Furthermore, a significant MCE is observed at sub-Kelvin temperatures under low magnetic fields, positioning $[Gd(NO_3)_3]\cdot 6H_2O$ among the leading Gd^{3+}-based candidates for ADR operation in this temperature regime.

II. MATERIALS AND METHODS

$[Gd(NO_3)_3]\cdot 6H_2O$ and $[Y(NO_3)_3]\cdot 6H_2O$ were obtained from commercial sources (Sigma-Aldrich, 99.90%) and used without further purification. Both materials crystallize in the triclinic space group *P*-1 (see CIF files with CCDC reference numbers 1 632 729 and 1 541 802, respectively). For the synthesis of 1% diluted polycrystalline powder of $[Gd@Y(NO_3)_3]\cdot 6H_2O$, 4.63 mg of $[Gd(NO_3)_3]\cdot 6H_2O$ (0.01 mmol) and 450.90 mg of $[Y(NO_3)_3]\cdot 6H_2O$ (1.18 mmol) were mixed and dissolved in the minimum volume of distilled water. The resulting solutions were dried under active vacuum. After several days, a white powder was obtained. All compounds remained structurally stable under our experimental conditions, with no indication of measurable dehydration.

Continuous-wave electron paramagnetic resonance (EPR) measurements on a 1% diluted polycrystalline sample of $[Gd@Y(NO_3)_3]\cdot 6H_2O$ were recorded using a Bruker Elexys 580 spectrometer operating in the X-band (9.715 GHz). The setup included an Oxford CF900 continuous gas-flow cryostat and a Mercury iTC temperature controller, which employed liquid helium for cooling and provided precise temperature regulation. A Bruker MD5 resonator was used with an external field modulation of 0.2 mT at 100 kHz. Spectra collected at 5 and 10 K were identical within experimental resolution. The microwave power was adjusted to avoid saturation effects, and the magnetic field was measured with a Bruker ER035 gaussmeter. Simulations of the spectra were performed with the EasySpin toolbox for MATLAB.[37]

Direct-current (DC) magnetic measurements on $[Gd(NO_3)_3]\cdot 6H_2O$ were performed on a Quantum Design MPMS-3 system. A polycrystalline powder sample (~5 mg) was loaded into a plastic capsule and immobilized with eicosane wax to prevent grain movement. Isothermal magnetization curves were collected in magnetic fields between 0 and 7 T over the temperature range 2–10 K. DC magnetic susceptibility data were recorded over the same temperature range under a constant applied magnetic field of $B = 0.1$ T. All data obtained were corrected for diamagnetic contributions coming from both the sample holder and eicosane wax. In addition, the complex alternating-current (AC) magnetic susceptibility, $\chi' - i\chi''$, was measured under zero applied magnetic field over the temperature range of 0.05–4 K, using a frequency of 525 Hz and an AC field amplitude of 2×10^{-4} T. Measurements were performed with a Quantum Design PPMS DynaCool equipped with the ^{3}He–^{4}He dilution refrigerator (DR) option. A thin pressed polycrystalline pellet (~6 mg) was prepared for these experiments, and susceptibility data were initially recorded in arbitrary units. Absolute values of the real component, χ', were obtained by comparison with DC susceptibility data collected with the MPMS-3 in the overlapping temperature range (2–4 K), where dissipative processes are negligible. The imaginary component, χ'', is reported in arbitrary units.

Heat capacity measurements on $[Gd(NO_3)_3]\cdot 6H_2O$ were carried out using the relaxation method in a Quantum Design PPMS equipped with a ^{3}He cryostat, covering temperatures down to 0.4 K under constant magnetic fields from 0 to 7 T. Additional measurements extended to 0.05 K under fields up to 1 T using a Quantum Design PPMS DynaCool with a DR module. The samples consisted of thin pressed polycrystalline pellets (~1 mg for ^{3}He and ~0.2 mg for DR). In both setups, Apiezon N grease (~0.1 mg) was applied to ensure good thermal contact between the sample and the calorimeter platform. Its contribution to the total heat capacity was subtracted using a phenomenological correction.

Direct quasi-adiabatic MCE measurements on $[Gd(NO_3)_3]\cdot 6H_2O$ were performed for complete demagnetization processes using the DR of the DynaCool. For these experiments, a pressed polycrystalline pellet of ~5 mg was mounted on a calorimeter platform coated with ~0.2 mg of Apiezon N grease to improve thermal coupling. In addition, the MCE of $[Gd(NO_3)_3]\cdot 6H_2O$ was also evaluated indirectly by applying standard thermodynamic relations to the measured magnetization and heat capacity data.

III. RESULTS AND DISCUSSION

A. Electron paramagnetic resonance

The zero-field splitting parameters for Gd^{3+} in $[Gd(NO_3)_3]\cdot 6H_2O$ were determined from EPR measurements by modeling the spectra with the spin Hamiltonian

$$\mathscr{H} = b_2^0\left(\frac{s_z}{\hbar}\right)^2 + \frac{b_2^2}{3}\left(\frac{s_x^2 - s_y^2}{\hbar^2}\right) - g_J\mu_B\vec{B}\cdot\left(\frac{\vec{s}}{\hbar}\right), \quad (1)$$

where $\vec{s}$ is the spin operator with quantum number $s = 7/2$. The parameters b_2^0 and b_2^2 represent the first-order zero-field splitting terms associated with axial and in-plane crystal-field anisotropy, respectively. Here, g_J is the Landé factor; μ_B is the Bohr magneton; and $\hbar$ is the reduced Planck constant. The three terms in Eq. (1) correspond to axial anisotropy, in-plane anisotropy, and the Zeeman interaction.

To minimize magnetic interactions that could otherwise hinder the determination of zero-field splitting parameters, EPR measurements were performed on diluted, isomorphous host matrices. This approach was first implemented by Misra and Mikolajczak,[38] who determined the anisotropy parameters of Gd^{3+} in $[Gd@R(NO_3)_3]\cdot 6H_2O$ single crystals for various trivalent host ions R. Particularly relevant are the results for 1% diluted $[Gd@Y(NO_3)_3]\cdot 6H_2O$ and $[Gd@Sm(NO_3)_3]\cdot 6H_2O$ since the ionic radius of Gd^{3+} lies between those of Y^{3+} and Sm^{3+}. The paramagnetic Sm^{3+} ion is an appropriate host because it undergoes rapid spin

10 April 2026 11:20:15

© Author(s) 2026

flips; viz., it has a very short spin-lattice relaxation time, rendering its interaction with Gd^{3+} negligible on the EPR timescale.[38,39]

The same study by Misra and Mikolajczak[38] revealed that b_2^0 and b_2^2 vary linearly with the host ionic radius and exhibit a temperature dependence. Since the present work focuses on the low-temperature properties of $[Gd(NO_3)_3]\cdot 6H_2O$, it is essential to determine these parameters at cryogenic temperatures. Among the hosts considered, only $[Gd@Sm(NO_3)_3]\cdot 6H_2O$ was previously investigated at liquid-helium temperatures, yielding $b_2^0/k_B = -0.095(1)$ K and $b_2^2/3k_B = 0.017$ K.[38] To complement these data, we conducted continuous-wave EPR experiments on a 1% diluted polycrystalline sample of $[Gd@Y(NO_3)_3]\cdot 6H_2O$ at liquid-helium temperatures (Fig. 1). The experimental spectrum is accurately reproduced, assuming $g_J = 2.0$, $b_2^0/k_B = -0.072(2)$ K, and $b_2^2/3k_B = 0.015(2)$ K.

Finally, the zero-field splitting parameters for Gd^{3+} in $[Gd(NO_3)_3]\cdot 6H_2O$ were estimated by linear interpolation between the values obtained for the Y^{3+} and Sm^{3+} hosts, yielding $b_2^0/k_B = -0.087(3)$ K and $b_2^2/3k_B = 0.016(2)$ K (Fig. 2). The ionic radii were taken from Ref. 40 for coordination number 6. These results confirm that the anisotropy is predominantly axial. Consequently, for $B = 0$, the 4 twofold-degenerate energy levels of Gd^{3+} in $[Gd(NO_3)_3]\cdot 6H_2O$ can be approximated by $s_z = \pm 7/2, \pm 5/2, \pm 3/2, \pm 1/2$, ordered from lowest to highest energy. The corresponding level spacings are comparable with those reported for other Gd^{3+} salts.[17,39,41]

B. Magnetization and magnetic susceptibility

Figure 3 shows the isothermal molar magnetization, M, of $[Gd(NO_3)_3]\cdot 6H_2O$ at selected temperatures. The experimental curves closely follow Brillouin-type behavior throughout the investigated temperature range. At 2 K and under high magnetic fields, the magnetization saturates at $7.0\, N_A\mu_B$, consistent with non-interacting Gd^{3+} ions characterized by $s = 7/2$ and $g_J = 2.0$.

Figure 4 shows the real, χ', and imaginary, χ'', components of the magnetic susceptibility of polycrystalline $[Gd(NO_3)_3]\cdot 6H_2O$ for temperatures below 1 K. The data strongly suggest the onset of antiferromagnetic ordering. A pronounced maximum in χ' occurs

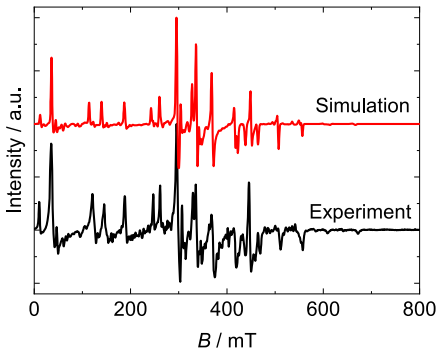

FIG. 1. Continuous-wave EPR spectra of Gd^{3+} on a 1% diluted polycrystalline sample of $[Gd@Y(NO_3)_3]\cdot 6H_2O$ at $T = 5$ K. Black line = experimental data; red line = simulation of a $s = 7/2$ spin system with $g_J = 2.0$ and crystal-field anisotropy parameters $b_2^0/k_B = -0.072$ K and $b_2^2/3k_B = 0.015$ K.

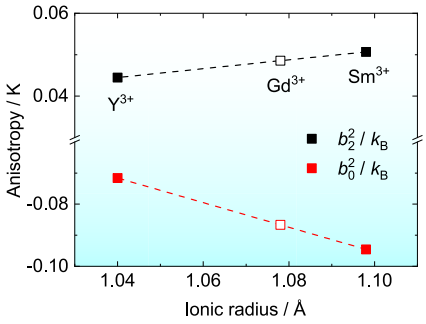

FIG. 2. Zero-field splitting parameters b_2^0/k_B and b_2^2/k_B for Gd^{3+} at liquid-helium temperatures as a function of the host ionic radius. The filled symbols represent values obtained from EPR measurements; the open symbols correspond to interpolated estimates.

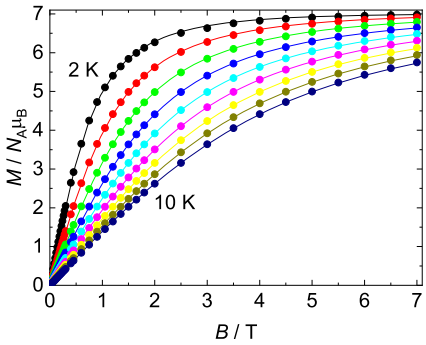

FIG. 3. Isothermal magnetization M of $[Gd(NO_3)_3]\cdot 6H_2O$ at selected temperatures. The filled symbols represent experimental data; the solid lines correspond to Brillouin-function fits.

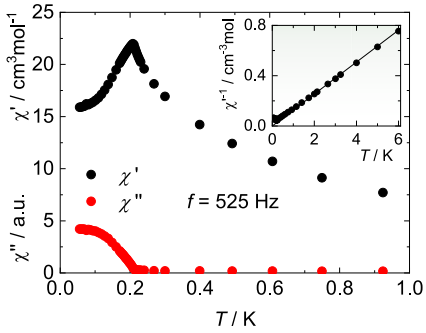

FIG. 4. Real (χ') and imaginary (χ'') components of the magnetic susceptibility of polycrystalline $[Gd(NO_3)_3]\cdot 6H_2O$ below 1 K. Inset: Inverse of the real component of the magnetic susceptibility, χ'^{-1}. The filled symbols represent experimental data; the solid line corresponds to the Curie–Weiss fit.

at the Néel temperature $T_N = 0.21$ K, reaching 22.0 $cm^3\ mol^{-1}$. Below T_N, χ' decreases gradually, while χ'' becomes non-zero, indicating the emergence of dissipative processes. The inverse susceptibility χ'^{-1} exhibits a linear temperature dependence down to 2 K, below which slight deviations from linearity appear, culmi-

10 April 2026 11:20:15

© Author(s) 2026

nating in an upward anomaly at $T_N = 0.21$ K, characteristic of an antiferromagnetic phase transition (inset of Fig. 4). The fit to the Curie–Weiss law $\chi'^{-1} = (T - \theta_W)/C$ yields the Curie constant of $C = 7.88(1)$ cm^3 K mol^{-1}, in excellent agreement with the expected value for non-interacting Gd^{3+} ions and the Weiss temperature $\theta_W = -0.02(1)$ K. This nearly vanishing Weiss temperature is fully consistent with previous reports.[34,35]

C. Heat capacity

Figure 5 presents the heat capacity, c_p, of $[Gd(NO_3)_3] \cdot 6H_2O$. At zero applied magnetic field, a pronounced λ-type anomaly appears at $T_N = 0.21$ K, coinciding with the Néel temperature identified from magnetic susceptibility measurements. This anomaly shifts to lower temperatures under small applied fields (see the inset of Fig. 5), consistent with antiferromagnetic ordering. Below T_N, c_p decreases exponentially, as expected for an antiferromagnetic ground state with a crystal-field anisotropy-induced energy gap.[42] At the lowest temperatures, a slight upturn in c_p is observed, most likely arising from hyperfine contributions associated with the ^{155}Gd and ^{157}Gd isotopes (combined natural abundance ≈30%), both of which possess nuclear spin $I = 3/2$. Notably, assuming an isotropic hyperfine interaction of the form $\mathscr{H} = A\vec{I} \cdot \vec{s}/\hbar^2$, a coupling constant $A = 0.8$ mK satisfactorily accounts for the anomaly (Fig. 5, dashed line). This value of A is consistent with hyperfine parameters reported for Gd^{3+} in various host matrices.[43]

A broad Schottky-like anomaly is observed underneath the λ-type peak, likely arising from a combination of crystal-field anisotropy and magnetic interactions. To clarify its origin, we analyzed the high-temperature tail of this anomaly. For magnetic ions with spin s subjected to axial and in-plane crystal-field anisotropy parameters b_2^0 and b_2^2, the high-temperature expansion of the heat capacity is given by

$$\frac{c_{cf}T^2}{R} = \frac{s(s+1)(2s+3)(2s-1)\left[(b_2^0)^2 + \frac{1}{3}(b_2^2)^2\right]}{45k_B^2}, \quad (2)$$

as derived in Ref. 44. For Gd^{3+} ions with $s = 7/2$ and zero-field splitting parameters $b_2^0/k_B = -0.087$ K and $b_2^2/3k_B = 0.016$ K, as determined for $[Gd(NO_3)_3] \cdot 6H_2O$, the calculated value is $c_{cf}T^2/R = 0.17$ K^2. The dipolar contribution to the Schottky-like tail can also be estimated. Following the van Vleck formalism,[45] the high-temperature expansion of the dipolar term is

$$\frac{c_{dip}T^2}{R} = \frac{Q\tau^2}{6}, \quad (3)$$

where $\tau = N_s g_J^2 \mu_B^2 s(s+1)/k_B$ is a characteristic temperature and $Q = N_s^{-2} \sum_m 2r_{nm}^{-6}$ is a geometrical factor. Here, N_s denotes the number of spins per unit volume. From the crystal structure of $[Gd(NO_3)_3] \cdot 6H_2O$, we estimate $N_s = 3.23 \times 10^{21}$ Gd^{3+} ions/cm^3 and $Q = 18.2$, yielding $\tau = 0.12$ K and $c_{dip}T^2/R = 0.05$ K^2. Combining crystal-field anisotropy and dipolar contributions gives a total $c_{cf}T^2/R + c_{dip}T^2/R = 0.22$ K^2, in excellent agreement with experiment (Fig. 5, black solid line). These results indicate negligible exchange interactions, supporting that antiferromagnetic ordering originates from dipolar coupling. This behavior closely resembles that observed in other well-known classical salts, such as $[GdCl_3] \cdot 6H_2O$ and $[Gd_2(SO_4)_3] \cdot 8H_2O$.[17]

External magnetic fields of $B \geq 1$ T are sufficient to suppress both crystal-field anisotropy and dipolar interactions, allowing the heat capacity to be accurately described by simple paramagnetic Schottky contributions (Fig. 5, colored solid lines). At the highest temperatures, the dominant contribution arises from lattice vibrations, which follow a Debye law that simplifies to $c_{latt}/T^3R = 6.3 \times 10^{-4}$ K^{-3} below 6 K (Fig. 5, dotted line).

The absolute entropy for different magnetic fields was derived from the heat capacity data using $S = \int [c_p/T]dT$ (Fig. 6). At zero applied field, the entropy saturates at $S = R\ln(2s+1) = 2.08R$ for $s = 7/2$ ions at 2 K, corresponding to 38.3 J kg^{-1} K^{-1} for $[Gd(NO_3)_3] \cdot 6H_2O$. Notably, at the antiferromagnetic transition temperature $T_N = 0.21$ K, the entropy is approximately $S \approx R\ln(2) = 0.69R$, indicating that only the lowest doublet ($s_z = \pm 7/2$) remains populated at the onset of magnetic ordering.

D. Magnetocaloric effect

The MCE of $[Gd(NO_3)_3] \cdot 6H_2O$ was evaluated using both direct measurements and indirect methods, based on thermodynamic relations.

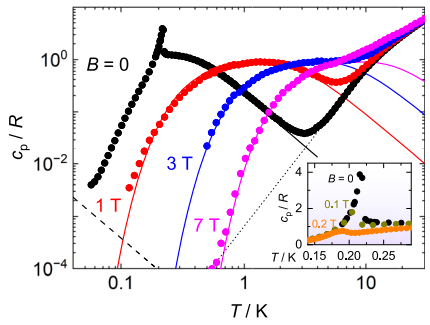

FIG. 5. Temperature dependence of the heat capacity c_p of $[Gd(NO_3)_3] \cdot 6H_2O$ for selected magnetic fields. Inset: Low-temperature c_p under small applied magnetic fields. The filled symbols represent experimental data; the solid lines correspond to calculated values; the dotted line indicates the lattice heat capacity; and the dashed line represents the hyperfine contribution.

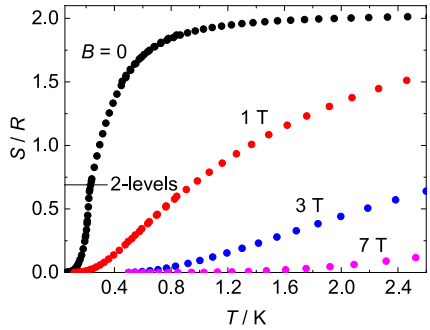

FIG. 6. Entropy S of $[Gd(NO_3)_3] \cdot 6H_2O$ at selected magnetic fields. The horizontal line marks the entropy expected for a two-level system.

10 April 2026 11:20:15

© Author(s) 2026

1. Direct measurements

Direct MCE measurements are presented in Fig. 7 for demagnetization processes starting at $B = 1$ T and bath temperatures of 0.3, 0.5 and 1 K. The plotted temperature traces are not corrected for heat exchange with the thermal bath; however, such heat leakage is negligible under our experimental conditions. At 0.1 K, the sample heat capacity is $c_{\text{sample}} \approx 10\ \mu\text{J K}^{-1}$, whereas the thermal conductance of the wires connecting the calorimeter platform to the bath is $G \approx 2$ nW K^{-1}, yielding a thermal time constant $\tau \approx c_{\text{sample}}/G = 5000$ s. Since the field-change events in the direct MCE measurements last roughly 30 s, i.e., much shorter than τ, the sample-platform assembly remains effectively thermally isolated during the sweep. As a result, the measured temperature traces provide an accurate representation of the adiabatic response of $[Gd(NO_3)_3] \cdot 6H_2O$.

At the highest magnetic fields and temperatures, the sample cools linearly, as expected for a paramagnet. A plateau is eventually reached as crystal-field anisotropy and dipolar interactions begin to dominate over the Zeeman effect. In addition, anomalies in the form of minima emerge when the material undergoes antiferromagnetic ordering, most prominently during demagnetization from 0.3 K. A minimum temperature of $T \simeq 0.15$ K is experimentally reached at $B = 0.4$ T at the transition, below which an inverted MCE occurs. As expected, the MCE vanishes once $[Gd(NO_3)_3] \cdot 6H_2O$ becomes magnetically ordered.

The quasi-adiabatic temperature traces, together with the heat-capacity data, enable construction of the $B - T$ phase diagram (Fig. 7). Both methods yield fully consistent results for the transition line separating the antiferromagnetic and paramagnetic phases. This boundary is satisfactorily described by the quadratic dependence $T_N(B) = T_N(0) - \alpha B^2$, as expected for an antiferromagnet sufficiently far from the critical-field region. Although this quadratic approximation is not expected to remain valid very close to the critical field, our data suggest a critical field of roughly $B_c \lesssim 1$ T for this material.

2. Indirect evaluation

The isothermal magnetic entropy change, ΔS_m, was calculated from the entropy curves (Fig. 6) for any magnetic field variation $\Delta B = B - 0$. In addition, ΔS_m was independently estimated from the magnetization data (Fig. 3), using the Maxwell relation $\Delta S_m = \int [\partial M/\partial T] dB$, yielding nearly identical results (Fig. 8, top panel). The adiabatic temperature change, ΔT_{ad}, associated with full demagnetization, was also evaluated from the entropy data (Fig. 8, bottom panel).

For the largest magnetic field change of $\Delta B = 7$ T, the maximum isothermal magnetic entropy change reaches $-\Delta S_m = 36.0$ J kg^{-1} K^{-1} at 1.5 K, while the corresponding adiabatic temperature change is as high as $\Delta T_{ad} = 13.3$ K at $T = 1.1$ K. Even for smaller magnetic field changes, the MCE remains substantial. For example, for $\Delta B = 1$ T, an entropy change of $-\Delta S_m = 26.1$ J kg^{-1} K^{-1} is observed at 0.6 K, corresponding to 68% of the total available magnetic entropy. The associated adiabatic temperature change reaches $\Delta T_{ad} = 5.0$ K at $T = 1.6$ K for the same magnetic field change.

These results clearly outperform many Gd^{3+}-based compounds in the sub-Kelvin range. In most cases, competing materials undergo magnetic phase transitions at relatively high temperatures (typically $\gtrsim 0.5$ K), which drastically reduces the available magnetic entropy and causes the MCE to vanish. Representative examples include $GdLiF_4$,[11] $Gd(HCOO)_3$,[12] $GdPO_4$,[13] GdF_3,[14] $GdVO_4$,[15] and $Gd(OH)F_2$,[16] as well as $Gd_3Ga_5O_{12}$ (GGG), whose MCE, despite its very low ordering temperature, drops sharply between 1 and 0.8 K due to the onset of short-range correlations.[46]

In contrast, $[Gd(NO_3)_3] \cdot 6H_2O$ remains one of the most competitive refrigerants for very low temperatures. Notably, it exhibits the highest reported adiabatic temperature change, ΔT_{ad}, together with the lowest temperature of its corresponding maximum, $T_{\Delta T}^{\max}$, for small field changes, such as $\Delta B = 1$ T, among state-of-the-art sub-Kelvin Gd^{3+}-based compounds (Table I). This exceptional performance stems from its extremely low magnetic ordering temperature, combined with a high magnetic density and remarkable lattice rigidity, with the latter reflected in its unusually small lattice heat

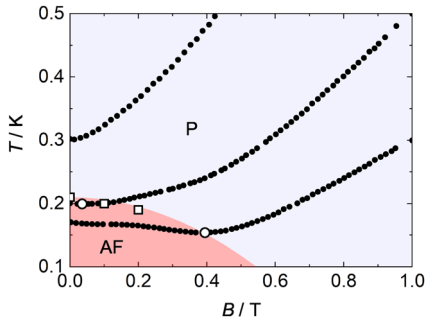

FIG. 7. Direct MCE measurements and $B - T$ phase diagram of $[Gd(NO_3)_3] \cdot 6H_2O$ in the $B - T$ plane, showing the boundary between the antiferromagnetic (AF) and paramagnetic (P) phases. Data points were obtained from c_p measurements (squares) and quasi-adiabatic demagnetization processes (circles) starting at $B = 1$ T and bath temperatures of 0.3, 0.5, and 1 K.

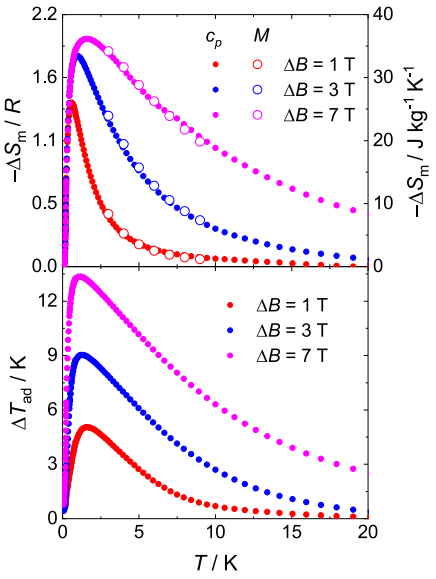

FIG. 8. Isothermal magnetic entropy change, ΔS_m (top), and adiabatic temperature change, ΔT_{ad} (bottom), for selected magnetic field changes, as obtained from heat capacity data (filled symbols) and magnetization data (open symbols).

10 April 2026 11:20:15

© Author(s) 2026

TABLE I. Comparison of Gd^{3+}-based magnetocaloric refrigerants for very low temperatures. Reported values include Néel or Curie temperature (T_N or T_C); magnetic entropy change ($-\Delta S_m$) for ΔB = 1 T; temperature at which $-\Delta S_m$ is maximum ($T_{\Delta S}^{max}$); adiabatic temperature change (ΔT_{ad}) for ΔB = 1 T; temperature at which ΔT_{ad} is maximum ($T_{\Delta T}^{max}$); relative cooling power ($RCP = |\Delta S_m| \times \delta T_{FWHM}$, where δT_{FWHM} is the full width at half maximum) for ΔB = 1 T; and lattice heat capacity parameter (c_{latt}/T^3R); literature reference. The units are indicated in parentheses. An ellipsis denotes an unknown value.

Compound	T_N or T_C (K)	$-\Delta S_m$ (J kg^{-1} K^{-1})	$T_{\Delta S}^{max}$ (K)	ΔT_{ad} (K)	$T_{\Delta T}^{max}$ (K)	RCP (J kg^{-1})	c_{latt}/T^3R (K^{-3})	References
$[GdCl_3] \cdot 6H_2O$	0.19	⋯	⋯	⋯	⋯	⋯	⋯	17
$[Gd_2(SO_4)_3] \cdot 8H_2O$	0.18	⋯	⋯	⋯	⋯	⋯	⋯	17
$\{Gd_2\}$	0.18	27.0	0.5	3.5	1.9	50	1.0×10^{-3}	18
$\{GdW_{10}\}$	0.036	2.3	0.8	⋯	⋯	5	2.0×10^{-3}	19
$\{GdW_{30}\}$	<0.01	1.5	0.3	⋯	⋯	2	1.1×10^{-2}	19
{GdZn}	<0.3	12.3	0.7	3.9	1.8	29	5.1×10^{-3}	20
$\{Gd_7\}$	<0.3	11.7	0.9	2.4	2.3	28	2.0×10^{-2}	21
Ba_2GdSbO_6	<0.4	⋯	⋯	⋯	⋯	⋯	4.8×10^{-6}	22
Sr_2GdSbO_6	<0.4	⋯	⋯	⋯	⋯	⋯	2.2×10^{-6}	22
$KBaGd(BO_3)_2$	0.24	14.3	0.5	⋯	⋯	20	⋯	23
$\{Gd_{12}Na_6\}$	<0.4	29.3	0.5	4.0	1.8	56	3.8×10^{-2}	24
$Gd_{9.33}[SiO_4]_6O_2$	<0.05	12.7	0.8	2.8	3.0	45	4.9×10^{-5}	25
$[Gd(NO_3)_3] \cdot 6H_2O$	0.21	26.1	0.6	5.0	1.6	46	6.3×10^{-4}	This work

capacity, c_{latt}/T^3R. Importantly, achieving large MCE values under small magnetic fields is highly desirable for practical applications, as it simplifies the design and fabrication of ADR's. Lower fields reduce the need for bulky superconducting magnets and complex cryogenic infrastructure, enabling more compact and cost-effective cooling systems.

IV. CONCLUSIONS

We have investigated the magnetothermal properties of the classical gadolinium salt $[Gd(NO_3)_3] \cdot 6H_2O$ down to temperatures approaching absolute zero. This compound undergoes an antiferromagnetic phase transition at T_N = 0.21 K, driven by weak dipolar interactions combined with dominant axial crystal-field anisotropy. These characteristics result in a very low operational temperature for $[Gd(NO_3)_3] \cdot 6H_2O$, which, together with its relatively high magnetic density and lattice stiffness, produces a remarkable magnetocaloric effect at very low temperatures.

ACKNOWLEDGMENTS

We thank Jesús I. Martínez for his assistance with the EPR experiments and acknowledge the Servicio General de Apoyo a la Investigación of Universidad de Zaragoza for technical support. This work was funded by EU (MSCA-DN MolCal, 101119865), MICIU/AEI/10.13039/501100011033/, and ERDF/EU (PID2024-159457OB-C21, CEX2023-001286-S).

AUTHOR DECLARATIONS

Conflict of Interest

The authors have no conflicts to disclose.

Author Contributions

David Gracia: Data curation (lead); Investigation (equal); Methodology (equal); Writing – original draft (lead); Writing – review & editing (equal). **Marc Ubach I Cervera**: Data curation (supporting); Investigation (equal); Methodology (equal); Writing – review & editing (equal). **Emmanouil K. Charkiolakis**: Data curation (supporting); Investigation (equal); Methodology (equal); Writing – review & editing (equal). **Inés García-Rubio**: Investigation (equal); Methodology (equal); Writing – review & editing (equal). **Constantinos J. Milios**: Investigation (equal); Methodology (equal); Writing – review & editing (equal). **Marco Evangelisti**: Conceptualization (lead); Data curation (supporting); Funding acquisition (lead); Investigation (equal); Methodology (equal); Supervision (lead); Writing – original draft (supporting); Writing – review & editing (equal).

DATA AVAILABILITY

All data presented in this article can be retrieved at https://doi.org/10.20350/digitalCSIC/17747.

REFERENCES

[1] A. M. Tishin and Y. I. Spichkin, *The Magnetocaloric Effect and its Applications* (CRC Press, 2016).
[2] V. K. Pecharsky and K. A. Gschneidner, "Magnetocaloric effect and magnetic refrigeration," J. Magn. Magn. Mater. **200**, 44 (1999).
[3] W. F. Giauque and D. P. MacDougall, "Attainment of temperatures below 1° absolute by demagnetization of $Gd_2(SO_4)_3 \cdot 8H_2O$," Phys. Rev. **43**, 768 (1933).
[4] F. Pobell, *Matter and Methods at Low Temperatures* (Springer-Verlag, 2013).
[5] P. J. Shirron, E. R. Canavan, M. J. DiPirro, J. G. Tuttle, and C. J. Yeager, "A multi-stage continuous-duty adiabatic demagnetization refrigerator," in *Advances in Cryogenic Engineering*, edited by Q.-S. Shu (Springer, Boston, 2000), p. 1629.

10 April 2026 11:20:15

© Author(s) 2026

[6]A. Cho, "Helium-3 shortage could put freeze on low-temperature research," Science **326**, 778 (2009).
[7]R. Stone, "Researchers rise to challenge of replacing helium-3," Science **353**, 15 (2016).
[8]V. Franco, J. S. Blázquez, J. J. Ipus, J. Y. Law, L. M. Moreno-Ramírez, and A. Conde, "Magnetocaloric effect: From materials research to refrigeration devices," Prog. Mater. Sci. **93**, 112 (2018).
[9]M. Evangelisti and E. K. Brechin, "Recipes for enhanced molecular cooling," Dalton Trans. **39**, 4672 (2010).
[10]B. Daudin, R. Lagnier, and B. Salce, "Thermodynamic properties of the gadolinium gallium garnet, $Gd_3Ga_5O_{12}$, between 0.05 and 25 K," J. Magn. Magn. Mater. **27**, 315 (1982).
[11]T. Numazawa, K. Kamiya, P. Shirron, M. DiPirro, and K. Matsumoto, "Magnetocaloric effect of polycrystal $GdLiF_4$ for adiabatic magnetic refrigeration," AIP Conf. Proc. **850**, 1579 (2006).
[12]G. Lorusso, J. W. Sharples, E. Palacios, O. Roubeau, E. K. Brechin, R. Sessoli, A. Rossin, F. Tuna, E. J. L. McInnes, D. Collison, and M. Evangelisti, "A dense metal-organic framework for enhanced magnetic refrigeration," Adv. Mater. **25**, 4653 (2013).
[13]E. Palacios, J. A. Rodríguez-Velamazán, M. Evangelisti, G. J. McIntyre, G. Lorusso, D. Visser, L. J. de Jongh, and L. A. Boatner, "Magnetic structure and magnetocalorics of $GdPO_4$," Phys. Rev. B **90**, 214423 (2014).
[14]Y. C. Chen, J. Prokleška, W. J. Xu, J. L. Liu, J. Liu, W. X. Zhang, J. H. Jia, V. Sechovský, and M. L. Tong, "A brilliant cryogenic magnetic coolant: Magnetic and magnetocaloric study of ferromagnetically coupled GdF_3," J. Mater. Chem. C **3**, 12206 (2015).
[15]E. Palacios, M. Evangelisti, R. Sáez-Puche, A. J. Dos Santos-García, F. Fernández-Martínez, C. Cascales, M. Castro, R. Burriel, O. Fabelo, and J. A. Rodríguez-Velamazán, "Magnetic structures and magnetocaloric effect in RVO_4 (R = Gd, Nd)," Phys. Rev. B **97**, 214401 (2018).
[16]Q. Xu, B. Liu, M. Ye, G. Zhuang, L. Long, and L. Zheng, "$Gd(OH)F_2$: A promising cryogenic magnetic refrigerant," J. Am. Chem. Soc. **144**, 13787 (2022).
[17]R. F. Wielinga, J. Lubbers, and W. J. Huiskamp, "Heat capacity singularities in two gadolinium salts below 1 K," Physica **37**, 375 (1967).
[18]M. Evangelisti, O. Roubeau, E. Palacios, A. Camón, T. N. Hooper, E. K. Brechin, and J. J. Alonso, "Cryogenic magnetocaloric effect in a ferromagnetic molecular dimer," Angew. Chem., Int. Ed. **50**, 6606 (2011).
[19]M. J. Martínez-Pérez, O. Montero, M. Evangelisti, F. Luis, J. Sesé, S. Cardona-Serra, and E. Coronado, "Fragmenting gadolinium: Mononuclear polyoxometalate-based magnetic coolers for ultra-low temperatures," Adv. Mater. **24**, 4301 (2012).
[20]J. Ruiz, G. Lorusso, M. Evangelisti, E. K. Brechin, S. J. A. Pope, and E. Colacio, "Closely-related $Zn^{II}_2Ln^{III}_2$ complexes (Ln^{III} = Gd, Yb) with either magnetic refrigerant or luminescent single-molecule magnet properties," Inorg. Chem. **53**, 3586 (2014).
[21]E. M. Pineda, G. Lorusso, K. H. Zangana, E. Palacios, J. Schnack, M. Evangelisti, R. E. P. Winpenny, and E. J. L. McInnes, "Observation of the influence of dipolar and spin frustration effects on the magnetocaloric properties of a trigonal prismatic $\{Gd_7\}$ molecular nanomagnet," Chem. Sci. **7**, 4891 (2016).
[22]E. C. Koskelo, C. Liu, P. Mukherjee, N. D. Kelly, and S. E. Dutton, "Free-spin dominated magnetocaloric effect in dense Gd^{3+} double perovskites," Chem. Mater. **34**, 3440 (2022).
[23]A. Jesche, N. Winterhalter-Stocker, F. Hirschberger, A. Bellon, S. Bachus, Y. Tokiwa, A. A. Tsirlin, and P. Gegenwart, "Adiabatic demagnetization cooling well below the magnetic ordering temperature in the triangular antiferromagnet $KBaGd(BO_3)_2$," Phys. Rev. B **107**, 104402 (2023).
[24]T. G. Tziotzi, D. Gracia, S. J. Dalgarno, J. Schnack, M. Evangelisti, E. K. Brechin, and C. J. Milios, "A $\{Gd_{12}Na_6\}$ molecular quadruple-wheel with a record magnetocaloric effect at low magnetic fields and temperatures," J. Am. Chem. Soc. **145**, 7743 (2023).
[25]Z. W. Yang, J. Zhang, B. Liu, X. Zhang, D. Lu, H. Zhao, M. Pi, H. Cui, Y. J. Zeng, Z. Pan *et al.*, "Exceptional magnetocaloric responses in a gadolinium silicate with strongly correlated spin disorder for sub-kelvin magnetic cooling," Adv. Sci. **11**, 2306842 (2024).
[26]J. A. Barclay and W. A. Steyert, "Materials for magnetic refrigeration between 2 K and 20 K," Cryogenics **22**, 73 (1982).
[27]Y. Yang, Q. C. Zhang, Y. Y. Pan, L. S. Long, and L. S. Zheng, "Magnetocaloric effect and thermal conductivity of $Gd(OH)_3$ and $Gd_2O(OH)_4(H_2O)_2$," Chem. Commun. **51**, 7317 (2015).
[28]J. Černák, K. Harčárová, M. Uličný, R. Tarasenko, M. Orendáč, and L. R. Falvello, "Syntheses, crystal structure and magnetocaloric effect of $[Gd(PDOA)(NO_3)(H_2O)_2]_n$," J. Mol. Struct. **1137**, 179 (2017).
[29]C. Li, G. O. Barasa, Y. Qiu, and S. Yuan, "Magnetocaloric effect and sign reversal of magnetic entropy change across the spin reorientation temperature in $R_3Fe_5O_{12}$ (R = Gd, Dy)," J. Alloys Compd. **820**, 153138 (2020).
[30]B. L. Liu, Q. F. Xu, L. S. Long, and L. S. Zheng, "Magnetocaloric effect of two Gd-based frameworks," Inorganics **10**, 91 (2022).
[31]Y. Q. Zhai, W. P. Chen, M. Evangelisti, Z. Fu, and Y. Z. Zheng, "Gd-based molecular coolants: Aggregating for better magnetocaloric effect," Aggregate **5**, 520 (2024).
[32]Meenakshi, S. Saini, N. Panwar, Ramovatar, and S. Kumar, "Giant magnetocaloric properties of Gd-based double perovskite compounds in cryogenic temperature range," J. Magn. Magn. Mater. **614**, 172766 (2025).
[33]D. Borah, N. B. Sankarammal, H. Goyal, S. S. Nagarkar, and M. Shanmugam, "Investigation of Gd(III) 2D metal-organic frameworks for magnetic refrigeration," Inorg. Chem. **64**, 14651 (2025).
[34]R. Kawashima and H. Isoda, "Temperature dependence of magnetic susceptibility in gadolinium nitrate crystal," Phys. Status Solidi A **145**, 59 (1994).
[35]R. Kawashima and H. Isoda, "Magnetic properties of gadolinium nitrate crystal having metastable behaviour," J. Phys. Soc. Jpn. **64**, 682 (1995).
[36]T. E. Katila, V. K. Typpi, G. K. Shenoy, and L. Niinistö, "Mössbauer studies of Gd^{3+} compounds at very low temperatures," Solid State Commun. **11**, 1147 (1972).
[37]S. Stoll and A. Schweiger, "EasySpin, a comprehensive software package for spectral simulation and analysis in EPR," J. Magn. Reson. **178**, 42 (2006).
[38]S. K. Misra and P. Mikolajczak, "Systematics of EPR spectra of Gd^{3+} in rare-earth trinitrate hexahydrate hosts," J. Chem. Phys. **69**, 3093 (1978).
[39]V. M. Malhotra, H. D. Bist, and G. C. Upreti, "Electron paramagnetic resonance of Gd^{3+} in single crystals of some lanthanide trichloride hexahydrates," J. Magn. Reson. (1969) **27**, 439 (1977).
[40]R. D. Shannon, "Revised effective ionic radii and systematic studies of interatomic distances in halides and chalcogenides," Acta Cryst. A **32**, 751–767 (1976).
[41]V. M. Malhotra, H. D. Bist, and G. C. Upreti, "Host lattice effects in the EPR spectra of Gd^{3+} ion in some hydrated lanthanide sulfates," J. Chem. Phys. **69**, 1919 (1978).
[42]L. J. De Jongh and A. R. Miedema, "Experiments on simple magnetic model systems," Adv. Phys. **50**, 947 (2001).
[43]A. Borel, H. Kang, C. Gateau, M. Mazzanti, R. B. Clarkson, and R. L. Belford, "Variable temperature and EPR frequency study of two aqueous Gd(III) complexes with unprecedented sharp lines," J. Phys. Chem. A **110**, 12434–12438 (2006).
[44]A. Abragam and B. Bleaney, *Electron Paramagnetic Resonance of Transition Ions* (Oxford University Press, 2012).
[45]J. H. Van Vleck, "The influence of dipole-dipole coupling on the specific heat and susceptibility of a paramagnetic salt," J. Chem. Phys. **5**, 320 (1937).
[46]M. Kleinhans, K. Eibensteiner, J. C. Leiner, C. Resch, L. Worch, M. A. Wilde, J. Spallek, A. Regnat, and C. Pfleiderer, "Magnetocaloric properties of $R_3Ga_5O_{12}$ (R = Tb, Gd, Nd, Dy)," Phys. Rev. Appl. **19**, 014038 (2023).

10 April 2026 11:20:15

© Author(s) 2026